# Uronate Isomerase: A Nonhydrolytic Member of the Amidohydrolase Superfamily with an Ambivalent Requirement for a Divalent Metal Ion†

LaKenya Williams, Tinh Nguyen, Yingchun Li, Tamiko N. Porter, and Frank M. Raushel*

*Department of Chemistry, P.O. Box 30012, Texas A&M University, College Station, Texas 77842-3012*

*Received March 16, 2006; Revised Manuscript Received April 26, 2006*

ABSTRACT: Uronate isomerase, a member of the amidohydrolase superfamily, catalyzes the isomerization of D-glucuronate and D-fructuronate. During the interconversion of substrate and product the hydrogen at C2 of D-glucuronate is transferred to the *pro-R* position at C1 of the product, D-fructuronate. The exchange of the transferred hydrogen with solvent deuterium occurs at a rate that is 4 orders of magnitude slower than the interconversion of substrate and product. The enzyme catalyzes the elimination of fluoride from 3-deoxy-3-fluoro-D-glucuronate. These results have been interpreted to suggest a chemical reaction mechanism in which an active site base abstracts the proton from C2 of D-glucuronate to form a *cis*-enediol intermediate. The conjugate acid then transfers this proton to C1 of the *cis*-enediol intermediate to form D-fructuronate. The loss of fluoride from 3-deoxy-3-fluoro-D-glucuronate is consistent with a stabilized carbanion at C2 of the substrate during substrate turnover. The slow exchange of the transferred hydrogen with solvent water is consistent with a shielded conjugate acid after abstraction of the proton from either D-glucuronate or D-fructuronate during the isomerization reaction. This conclusion is supported by the competitive inhibition of the enzymatic reaction by D-arabinaric acid and the monohydroxamate derivative with $K_i$ values of 13 and 670 nM, respectively. There is no evidence to support a hydride transfer mechanism for uronate isomerase. The wild type enzyme was found to contain 1 equiv of zinc per subunit. The divalent cation could be removed by dialysis against the metal chelator, dipicolinate. However, the apoenzyme has the same catalytic activity as the Zn-substituted enzyme and thus the divalent metal ion is not required for enzymatic activity. This is the only documented example of a member in the amidohydrolase superfamily that does not require one or two divalent cations for enzymatic activity.

The amidohydrolase (AH[1]) enzyme superfamily catalyzes predominantly the hydrolysis of amide and ester functional groups attached to carbon or phosphorus centers within a diverse set of amino acid, sugar, and nucleic acid substrates (*1*, *2*). Well-characterized enzymes within this superfamily include phosphotriesterase (*3*), urease (*4*), dihydroorotase (*5*), and adenosine deaminase (*6*) among others. One of the most diverged members of this enzyme superfamily is uronate isomerase (URI). This protein catalyzes one of the rare nonhydrolytic reactions for this superfamily. Uronate isomerase was initially identified as an enzyme within the AH superfamily from the structural characterization of URI from *Thermatoga maritima* (*7*) and subsequent amino acid sequence alignments (*8*). This enzyme catalyzes the isomerization of D-glucuronate to D-fructuronate in the first step of the metabolic pathway for the utilization of D-glucuronic acid. The chemical transformation is illustrated in Scheme 1. URI

Scheme 1

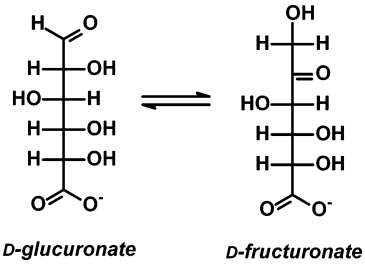


thus represents a rather intriguing example for the divergence of reaction specificity from ancestral proteins that share a common structural template.

All of the structurally characterized members of the AH superfamily contain a mononuclear or binuclear metal center that is embedded within the enzyme active site and possess a $(\beta/\alpha)_8$ protein fold (*1*). The most highly conserved metal ligands in the AH superfamily include a His-Xaa-His motif from the end of $\beta$-strand 1, two histidines from the ends of $\beta$-strands 5 and 6, and an aspartate from the end of $\beta$-strand 8 (*1*). However, a sequence alignment of 36 uronate isomerases has unveiled the universal absence of a conserved histidine at the end of $\beta$-strand 6. This is the only documented example of a catalytically active member of the AH superfamily that does not contain a histidine at this location within the active site. The metal content of URI from *T. maritima* that was solved by X-ray diffraction methods was

† This work was supported in part by the National Institutes of Health (GM 33894 and GM 71790) and the Robert A. Welch Foundation (A-840). L.W. was supported by a predoctoral fellowship from NIH (F31 GM 77102).

* To whom correspondence may be addressed. Phone: (979)-845-3373. Fax: (979)-845-9452. E-mail: raushel@tamu.edu.

[1] Abbreviations: AH, amidohydrolase; MDH, mannonate dehydrogenase; MDT, mannonate dehydratase; URI, uronate isomerase; TEMPO, 2,2,6,6,-tetramethyl-1-piperidinyloxy; ICP-MS, inductively coupled plasma mass spectrometry; TIM, triosephosphate isomerase; PGI, phosphoglucose isomerase.

10.1021/bi060531l CCC: $33.50 
Published on Web 05/27/2006

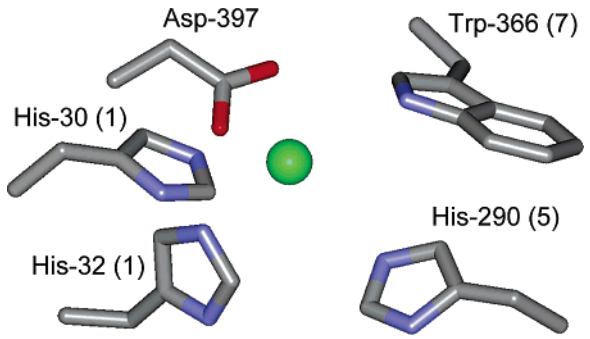


FIGURE 1: Representation of the active site of uronate isomerase from *T. maritima* (*7*). The coordinates were taken from the PDB file 1J5S. The green sphere has been modeled by the authors as a water molecule in the original publication (*7*).

not determined, but the extra electron density in the putative metal binding site was conservatively modeled as a water molecule (*7*). The orientation of this putative metal site with respect to the conserved active site ligands is presented in Figure 1. Metal ligation has been proposed to His-30, His-32, and Asp-397 (*7*). However, the interatomic distances from these residues to the putative metal ion in the active site are rather long: 2.8, 2.7, and 2.4 Å to His-30, His-32, and Asp-397, respectively. These results cast some uncertainty about the identity of the divalent cation and its role in the structure and function of URI.

The reaction catalyzed by URI is analogous to the isomerization of other aldose−ketose monosaccharide pairs. Enzymes catalyzing these 1,2-hydrogen transfers have been proposed to proceed via two general mechanisms as presented in Scheme 2. In the more common transformation, an active site base ($:B_1$) abstracts a proton from C2 of the aldose substrate and an active site acid ($H:B_2$) donates a proton to the carbonyl oxygen at C1 to generate an enediol intermediate. In the subsequent step the proton from C2 is transferred to C1 of the intermediate while a proton is abstracted from the hydroxyl at C2 to generate the ultimate ketose product. Alternatively, in an apparently more rare mechanism, an active site base ($:B_1$) abstracts a proton from the hydroxyl at C2 of the aldose, concomitant with a 1,2-hydride transfer from C2 to C1 and protonation of the carbonyl oxygen ($H:B_2$). Proton transfer mechanisms have been established for a number of enzymes including phosphoglucose isomerase (*9*) and triosephosphate isomerase (*10*−*14*). The most salient mechanistic probe for the proton transfer mechanism has been the enzyme-catalyzed exchange of the C2-hydrogen with solvent. With triosephosphate isomerase (TIM) this hydrogen exchanges with solvent at a rate that is an order of magnitude faster than the interconversion of substrate and product (*12*). In contrast, a hydride transfer mechanism has been proposed for the metalloenzyme, xylose isomerase, based upon the absence of a substrate/solvent hydrogen exchange reaction and the structural orientation of substrates and side chain substituents in the active site (*15*, *16*).

In this paper we report the cloning, expression, and purification of uronate isomerase from *Escherichia coli*. The purified protein contains 1 equiv of zinc per subunit that can be removed with metal chelators without the loss of catalytic activity. The proton at C2 of D-glucuronate is transferred stereospecifically to the *pro-R* hydrogen position at C1 of D-fructuronate. The enzyme catalyzes the elimination of fluoride from 3-deoxy-3-fluoro-D-glucuronate and the slow exchange of the hydrogen at C-2 of D-glucuronate with solvent water. These results are consistent with a proton transfer mechanism and a *cis*-enediol intermediate from an active site that does not require the presence of a divalent cation. This is the only example of an enzyme in the AH superfamily that does not require a divalent cation for catalytic activity.

## MATERIALS AND METHODS

*Materials.* D-Glucuronic acid was purchased from Acros Organics. Chromatography columns and resins used for protein purification were obtained from Amersham Biosciences. Wizard miniprep DNA purification kits were acquired from Promega. The Gene Technology Laboratory at Texas A&M University was the source of the oligonucleotide primers, and they were responsible for all of the DNA sequencing. Dialysis kits were purchased from Fisher, and all other compounds were obtained from Sigma-Aldrich. Dr. Wen Shan Yew constructed the expression plasmid for D-mannonate dehydratase from *Novosphingobium aromaticivorans*, which was a most generous gift from Professor John A. Gerlt of the University of Illinois.

*NMR Measurements.* $^1$H NMR spectra were acquired on a Varian Unity 500 or Inova 500 NMR spectrometer operating at frequency of 500 MHz. $^1$H NMR spectra were obtained using an 8000 Hz sweep width with a 3 s acquisition time and a 4 s relaxation delay between pulses. Decoupling experiments were acquired with decoupling powers not exceeding 20 dB. $^{19}$F NMR spectra were obtained on an Inova 400 NMR spectrometer operating at a frequency of 376 MHz. Spectra were acquired using a 120 kHz sweep width with a 1 s acquisition time and a 4 s relaxation delay. The $^{19}$F NMR spectra were referenced to $CCl_3F$ as an external standard at 0 ppm.

*Cloning and Purification of Uronate Isomerase.* The *uxa*C gene encoding *E. coli* uronate isomerase (gi: 16130987) was amplified by PCR and inserted into pET28 without a his-tag. The protein was expressed in the *E. coli* strain BL21-(DE3), and single colonies were used to inoculate 5 mL of LB medium supplemented with 50 $\mu$g/mL kanamycin. The overnight culture was used to inoculate 1 L of TB medium supplemented with 50 $\mu$g/mL kanamycin. The large culture was grown at room temperature until an $A_{600}$ of ∼0.4−0.6 was reached, and then 1.0 mM $ZnCl_2$ was added, followed by induction with 0.4 mM IPTG. The cells were incubated overnight and then centrifuged at 6000 rpm for 10 min at 4 °C. The cell pellet was resuspended in 50 mM HEPES, pH 8.0, and 500 $\mu$M $ZnCl_2$. The cells were lysed by sonication and the nucleic acids precipitated by dropwise addition of 2.0% (w/v) protamine sulfate solution. The solution was centrifuged at 12 000 rpm and the lysate fractioned between 50% and 80% saturation of ammonium sulfate. After centrifugation, the pellet was resuspended in a minimal amount of buffer (50 mM HEPES, pH 8.0), loaded onto a Superdex 200 gel filtration column, and eluted at a flow rate of 2.5 mL/min. Fractions containing uronate isomerase were identified by SDS−PAGE and activity assays. The pooled enzyme was loaded onto a Resource Q anion exchange column preequilibrated with buffer A (20 mM HEPES, pH

Scheme 2

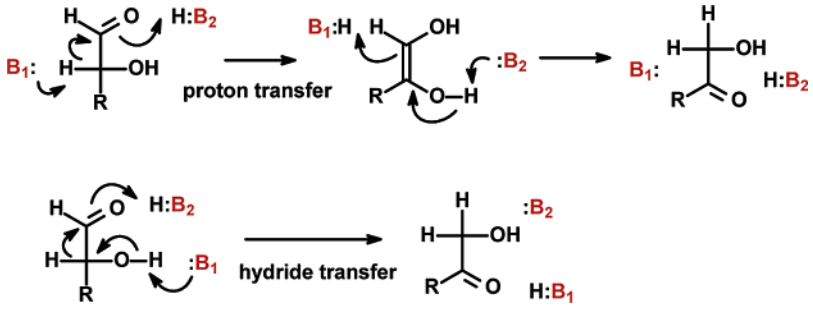


8.0) and eluted with a 0−30% gradient of buffer B (20 mM HEPES, pH 8.0 and 1.0 M NaCl) at a flow rate of 4.5 mL/min. The fractions were assayed and pooled based on the enzymatic activity. The purified enzyme was stored in the refrigerator at 4 °C for up to 1 year without significant loss of activity.

*Cloning and Purification of* D*-Mannonate Dehydrogenase.* The *uxu*B gene (gi: 26111644) from *E. coli* that encodes D-mannonate dehydrogenase (MDH) was cloned into a pET30 expression vector. The gene was transformed into BL21(DE3) and the cells grown in TB broth at 37 °C. D-Mannonate dehydrogenase was purified using the same methods previously described for the isolation of uronate isomerase, but no metal was added to the purification buffers. The cell extract was made 40−60% of saturation with ammonium sulfate, and the resuspended pellet was subjected to fractionation with the aid of a Superdex 200 gel filtration column. Fractions containing D-mannonate dehydrogenase were pooled, quick-frozen, and stored at −80 °C.

*Purification of* D*-Mannonate Dehydratase.* The expression plasmid for D-mannonate dehydratase (MDT) from *N. aromaticivorans* (gi: 48847978) was transformed into BL21(DE3) competent cells and streaked on a LB plate containing 50 $\mu$g/mL ampicillin. Single colonies were used to inoculate 5 mL of LB medium supplemented with ampicillin and incubated overnight at 25 °C. The fresh overnight culture was used to inoculate 3 L of LB supplemented with 100 $\mu$g/mL ampicillin. The culture was incubated at 25 °C for 48 h without induction. The culture was supplemented with ampicillin every 10 h. The cells were harvested and resuspended in 100 mL of buffer A, containing 5 mM imidazole, 500 mM NaCl, 5 mM $MgCl_2$, and 20 mM Tris-HCl pH 7.9. The cells were lysed by sonication and centrifuged at 13 000 rpm for 1 h. The cell lysate was applied to a Chelating Sepharose Fast Flow column in buffer solution A. The $Ni^{2+}$ affinity column was previously charged with 50 mM $NiSO_4$ and then washed with buffer solution A. After the cell lysate was applied to the column, it was washed with 200 mL of buffer solution A and 300 mL of 95% buffer B−5% buffer C. Buffer B contained 60 mM imidazole, 500 mM NaCl, 5 mM $MgCl_2$, and 20 mM Tris-HCl pH 7.9. Buffer C contained 1 M imidazole, 500 mM NaCl, 5 mM $MgCl_2$, and 20 mM Tris-HCl. The pooled enzyme was dialyzed against 20 mM $P_i$, pH 7.8, containing 5 mM $MgCl_2$ for a total of 8 h.

*Solvent Proton Exchange.* The ability of URI to incorporate solvent deuterium into the substrate and product was measured by NMR spectroscopy upon the addition of URI and D-glucuronate in $D_2O$. The 1.0 mL assay contained 5.0 mM D-glucuronate, 50 mM $P_i$ buffer, pD 8.0, and 10 $\mu$M uronate isomerase. $^1$H NMR spectra were collected every hour for 24 h, and the exchange was monitored at the $\alpha$-$H_1$ and $\beta$-$H_1$ resonances of D-glucuronate.

*Enzymatic Synthesis of 2-Keto-3-deoxy-*D*-gluconic acid.* D-Mannonate, 25 mM, 50 mM $P_i$ buffer, pH 7.8, 5 mM $MgCl_2$, and 700 nM D-mannonate dehydratase were incubated at room temperature overnight. The solution was passed through a 0.2 $\mu$m Corning syringe filter and then dried using a rotary evaporator. The solution was redissolved in 750 $\mu$L of 50 mM $P_i$, pD 8.0, for NMR analysis.

*Enzymatic Synthesis of 2-Keto-3-deoxy-*D*-[6-$^2$H]-gluconic Acid (**4**).* D-Glucuronate (**1**) (10 mM) was incubated with 20 $\mu$M uronate isomerase, 50 mM $P_i$, pD 8.0, in 99% $D_2O$. After 12 h the proton at C2 of D-glucuronate was 92% substituted with deuterium. D-Mannonate dehydrogenase (12 $\mu$M) was added to the solution with 10 mM NADH and 1 $\mu$M uronate isomerase to ensure complete enzymatic production of D-[1-$^2$H]-mannonic acid (**3**). After 4 h, the solution was checked by NMR. The mixture was filtered with a 0.2 $\mu$m Corning syringe filter and then treated with activated charcoal to remove any $NAD^+$/NADH. The D-[1-$^2$H]-mannonic acid (**3**) was incubated with 700 nM D-mannonate dehydratase, 50 mM $P_i$, pH 7.8, and 5 mM $MgCl_2$. After 8 h the formation of **4** was complete. The solution was dried using a rotary evaporator and the product dissolved in a buffer of $P_i$, pD 8.0. The enzymatic transformation is presented in Scheme 3.

*Synthesis of Arabinaric Acid*. The synthesis of D-arabinaric acid (**6**) and its monohydroxamate (**8**) derivative is summarized in Scheme 4. D-(+)-Arabinitiol (**5**), 3.0 g, and sodium nitrite (100 mg) were dissolved in nitric acid (15 mL, 70%). The mixture was heated in an oil bath at 85 °C for 16 h. After the nitric acid was removed by reduced pressure at 70 °C, a colorless solid (2.5 g, yield of ~80% from $^1$H NMR) of the two possible lactones was obtained. The crude product (0.5 g) was dissolved in water (50 mL) and titrated with sodium hydroxide (10 M) to pH 10. The solution was applied to a Dowex AG 1-X8 anion exchange column in the formate form. The column was washed with 300 mL of water, and then a linear gradient of 0 to 2 M formic acid was applied. Fractions containing the desired product were collected and condensed to dryness. The residue (0.35 g, 70% yield) was titrated to pH 10 with NaOH to provide the sodium salt of D-arabinaric acid (**6**) (also known as D-lyxaric acid). $^1$H NMR ($D_2O$): 4.05 ppm (1 H, $J$ = 1.4 Hz), 3.91 ppm (1 H, $J$ = 7.6 Hz), 3.88 ppm (1 H, $J_1$ = 7.6 Hz, $J_2$ = 1.4 Hz). $^{13}$C NMR ($D_2O$): 179.96, 179.41, 73.55, 73.52, and 72.25 ppm. MS ($M - H^+$): 179.0 (observed), 179.0 (calculated).

Scheme 3

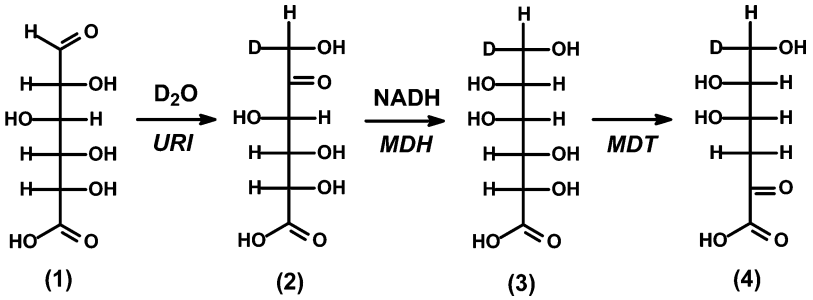


Scheme 4

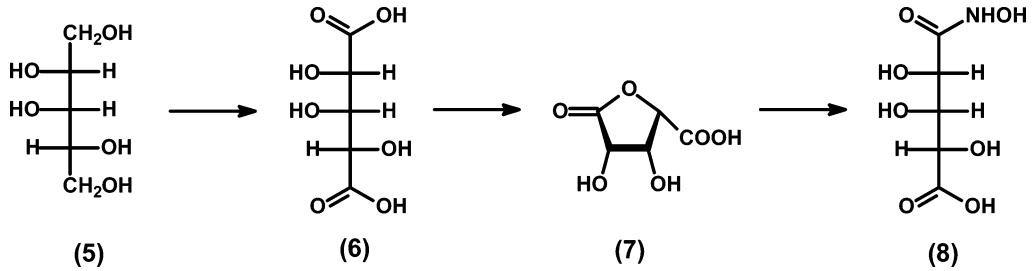


Scheme 5

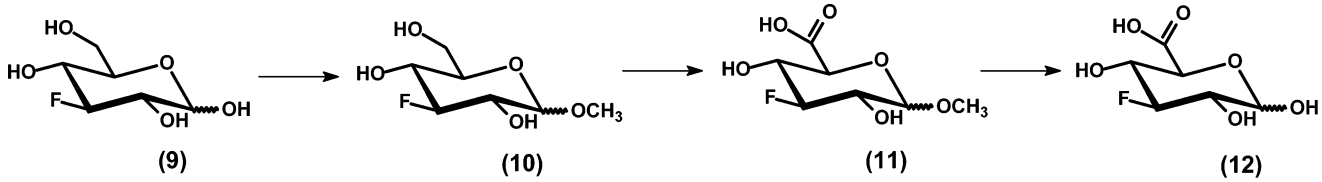


*Monohydroxamate of D-Arabinaric Acid.* The crude lactone mixture (1.8 g) from the oxidation of D-arabinitol as described above was dissolved in 5.0 mL of water. To this solution was added 4.0 mL of 50% hydroxylamine. The reaction mixture was stirred at room temperature for 1 h. The precipitate was collected by filtration and washed with cold water (1 mL × 2). The filtrate was condensed to about 3 mL and heated until a clear solution was formed. The solution was allowed to stand overnight to provide another portion of the crystalline product. Single crystals were obtained by recrystallization of the product from water and subjected to X-ray crystallographic structure analysis. The structure of the product was determined to be the hydroxylamine salt of (2*S*,3*R*,4*S*)-4-(hydroxycarbamoyl)-2,3,4-trihydroxybutanoate (**8**). $^1$H NMR ($D_2O$): 4.06 ppm (1 H, $J$ = 1.5 Hz), 3.92 ppm (1 H, $J$ = 8.5 Hz), 3.89 ppm (1 H, $J_1$ = 8.5 Hz, $J_2$ = 1.5 Hz). $^{13}$C NMR ($D_2O$): 178.68, 171.07, 72.52, 71.28, and 70.19 ppm. MS ($M - H^+$): 194.1 (observed), 194.0 (calculated).

*Synthesis of Methyl 3-Deoxy-3-fluoro-D-glucoside (**10**).* The synthesis of 3-deoxy-3-fluoro-D-glucuronic acid (**12**) is summarized in Scheme 5. The 3-deoxy-3-fluoro-D-glucose (**9**) was made according to the method of Tewson and Welch (*17*). A suspension of Dowex 50W X5-400 ($H^+$, 1.0 g, dry) in a solution of 3-deoxy-3-fluoro-D-glucose (1.02 g) in methanol (20 mL) was refluxed for 16 h. The resin was removed by filtration and washed with methanol (3 × 5 mL), and the combined fractions were condensed to dryness. The residue was subjected to flash silica gel chromatography with a methanol solution in chloroform (10%). The product (0.91 g, 83%) was a mixture of two methyl pyranosides (**10**) and two methyl furanosides (4:1 as estimated from the $^{19}$F NMR spectrum). $^{19}$F NMR for pyranoside: −191.1 ppm (dt, $J_1$ = 52.8 Hz, $J_2$ = 14.4 Hz), −194.9 ppm (dtd, $J_1$ = 52.8 Hz, $J_2$ = 56.2 Hz, $J_3$ = 4.0 Hz). $^{19}$F NMR for pyranoside: −199.2 ppm (ddd, $J_1$ = 51.4 Hz, $J_2$ = 16.6 Hz, $J_3$ = 12.5 Hz). The $^{19}$F NMR resonances for the two furanosides ranged from −199.3 to −198.8 ppm. MS ($M + Li^+$): 203.1 (observed), 203.1 (calculated).

*Synthesis of Methyl 3-Deoxy-3-fluoro-D-glucuronate (**11**).* Methyl 3-deoxy-3-fluoro-D-glucoside (**10**) (0.81 g, 4.1 mmol) and sodium bromide (0.32 g, 3.1 mmol) were dissolved in water (80 mL). Sodium hypochlorite (6 mL, 10−13% aqueous solution, 12 mmol) was added, and the pH was adjusted to 10 by the addition of HCl (1 M). TEMPO (2,2,6,6-tetramethyl-1-piperidinyloxy, 10 mg) was added to the reaction mixture and stirred. To keep the pH of the reaction mixture ∼10, NaOH (1 M) was added dropwise during the reaction. After 60 min, the pH of the solution stopped changing and the reaction was quenched with methanol (5 mL). After removal of solvent water under reduced pressure, the solid residue was washed with methanol 3 times. The methanol solutions were combined and condensed to dryness, and the residue was dissolved in water (20 mL) and passed through a column of Dowex 50W X8-400 ($H^+$). After elution with water the acidic fractions were combined and condensed to dryness to yield **11** as a colorless solid (0.78 g, 90%). $^{19}$F NMR ($D_2O$): −195.3 ppm (dt, $J_1$ = 52.0 Hz, $J_2$ = 13.0 Hz), −199.5 ppm (dtd, $J_1$ = 53.6 Hz, $J_2$ = 13.0 Hz, $J_3$ = 3.0 Hz). MS ($M-H^+$): 209.0 (observed), 209.0 (calculated).

*3-Deoxy-3-fluoro-D-glucuronic Acid.* Methyl 3-deoxy-3-fluoro-D-glucuronate (93 mg) was dissolved in aqueous HCl (37%). The resulting solution was stirred at 4 °C for

4.5 days, and then the reaction mixture was condensed to dryness. The residue was dissolved in water (50 mL) and purified on a DEAE-Sephadex anion exchange column ($HCO_3^-$ form). The compound was eluted with a 2.4 L gradient of sodium bicarbonate (10 mM to 80 mM). Fractions containing the fluorinated D-glucuronic acid were collected and condensed to dryness. The residue was treated with Dowex 50W X8-400 ($H^+$). The solution was condensed to dryness to yield 3-deoxy-3-fluoro-glucuronic acid (**12**) (70 mg, 80%). α-3-Deoxy-3-fluoro-glucuronic acid: $^1$H NMR ($D_2O$): 5.14 ppm (H1, t, $J_{H1-F} = 4.0$ Hz, $J_{H1-H2} = 4.0$ Hz), 4.48 ppm (H3, dt, $J_{H3-F} = 54.2$ Hz, $J_{H3-H2} = 9.15$ Hz, $J_{H3-H4} = 9.15$ Hz), 3.97 ppm (H5, $J_{H5-H4} = 10.24$ Hz), 3.71 ppm (H2, $J_{H2-F} = 13.40$ Hz, $J_{H2-H3} = 9.15$ Hz, $J_{H2-H1} = 4.0$ Hz), 3.67 ppm (H4, $J_{H4-F} = 13.4$ Hz, $J_{H4-H3} = 9.15$, $J_{H4-H5} = 10.24$ Hz). $^{19}$F NMR ($D_2O$): −199.85 ppm (dtd, $J_{F-H3} = 54.20$ Hz, $J_{F-H2} \approx$ JF−H4 ≈ 13.40 Hz, $J_{F-H1} = 4.0$ Hz). *β*-3-Deoxy-3-fluoro-glucuronic acid: $^1$H NMR ($D_2O$): 4.54 ppm (H1, d, $J_{H1-F} = 0.50$ Hz, $J_{H1-H2} = 7.83$ Hz), 4.30 ppm (H3, dt, $J_{H3-F} = 52.80$ Hz, $J_{H3-H2} = 8.81$ Hz, $J_{H3-H4} = 8.81$ Hz), 3.64 ppm (H4, $J_{H4-F} = 13.81$ Hz, $J_{H4-H3} = 8.81$, $J_{H4-H5} = 10.05$ Hz) 3.61 ppm (H5, $J_{H5-H4} = 10.05$ Hz), 3.43 ppm (H2, $J_{H2-F} = 13.81$ Hz, $J_{H2-H3} = 8.81$ Hz, $J_{H2-H1} = 7.83$ Hz). $^{19}$F NMR (m, in $D_2O$): −194.65 (dt, $J_{F-H3} = 52.80$ Hz, $J_{F-H2} \approx J_{F-H4} \approx 13.81$ Hz). MS ($M - H^+$): 195.0 (observed), 195.0 (calculated).

*Uronate Isomerase Activity Assays.* The conversion of D-glucuronate to D-fructuronate by uronate isomerase was coupled to the conversion of D-fructuronate and NADH to D-mannonate and $NAD^+$ by D-mannonate dehydrogenase (*18, 19*). The assay was monitored spectrophotometrically for the decrease in absorbance at 340 nm for the oxidation of NADH to $NAD^+$. The assay solution contained 50 mM HEPES, pH 8.0, 5 mM D-glucuronate, 0.2 mM NADH, 10 μM of dipicolinate (only for assay of the apoenzyme), 2 μM D-mannonate dehydrogenase, and uronate isomerase (1−10 nM) in a final volume of 250 μL. The values of $k_{cat}$, $K_a$, and $k_{cat}/K_a$ for the conversion of D-glucuronate to D-fructuronate were determined by variation of the D-glucuronate concentration (0.1 to 5.0 mM) and a fit of the velocity data to eq 1. The kinetic constants for the competitive inhibition of this enzyme by substrate analogues were obtained by a fit of the data to eq 2. In these equations, [A] is the substrate concentration and $K_{is}$ is the slope inhibition constant.

$$v/E_t = (k_{cat}[A])/(K_a + [A]) \quad (1)$$

$$v/E_t = (k_{cat}[A])/(K_a(1 + (I/K_{is})) + [A]) \quad (2)$$

*Metal Binding Studies.* The role of the putative metal ion in the function of uronate isomerase was investigated by analyzing the activity of the apoenzyme. Apo-URI was prepared by dialyzing 3.0 mL of 54 μM URI against 3 changes of 50 mM MES buffer (pH 6.0) containing 20 mM dipicolinate, for 3 days. Aliquots were removed periodically and assayed for catalytic activity. Dipicolinic acid was removed by dialyzing the enzyme against 50 mM metal-free HEPES buffer at pH 8.0 for 3 days. Apo-URI (18.5 μM) was reconstituted with 0.9 mM $Zn^{2+}$, $Co^{2+}$, $Mn^{2+}$, $Ni^{2+}$, or $Cd^{2+}$, in 50 mM HEPES buffer, pH 8.0 and the kinetic parameters were determined for the reconstituted enzymes. The metal content of all enzyme derivatives was quantified by ICP-MS at the Elemental Analysis Laboratory at Texas A&M University. The concentration of enzyme was determined by Bradford assays (*20*).

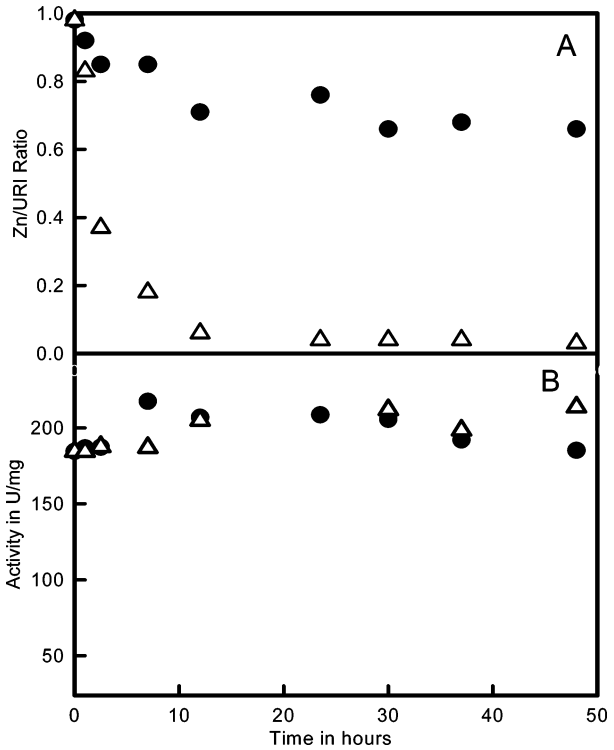


FIGURE 2: (A) The zinc content of uronate isomerase during dialysis against the metal chelator, dipicolinic acid (Δ) versus the control (●) at pH 8.0. The zinc content was determined via ICP-MS. (B) The catalytic activity of uronate isomerase during the dialysis against the metal chelator (Δ) and the control (●).

## RESULTS

*Kinetic Constants for Uronate Isomerase.* The uronate isomerase from *E. coli* was purified to homogeneity using ammonium sulfate fractionation, gel filtration, and ion exchange chromatography. The purified enzyme was found to contain 0.87 equiv of $Zn^{2+}$ per subunit. At pH 8.0 the values of $k_{cat}$, $K_a$, and $k_{cat}/K_a$ were found to be 196 ± 6 $s^{-1}$, 0.51 ± 0.05 mM, and 3.8 (±0.4) × $10^5$ $M^{-1}$ $s^{-1}$.

*Metal Binding Studies.* The catalytic efficiency of uronate isomerase in the absence or presence of an enzyme-bound divalent cation was investigated by removal of the zinc with the metal chelator, dipicolinic acid. The bound metal content was quantified by ICP-MS and the catalytic activity determined periodically after the initiation of dialysis with the metal chelator. The $Zn^{2+}$ content was diminished to less than 0.05 per subunit after 24 h of dialysis as shown in Figure 2A. In the absence of added chelator the metal content dropped to ∼0.6 per subunit after 2 days of dialysis. The catalytic activity of URI did not decrease, either in the presence or in the absence of the metal chelator as illustrated in Figure 2B. These data demonstrate that URI can bind up to 1 equiv of $Zn^{2+}$ but that the metal ion is not critical for catalytic activity. Dialysis of URI in the presence of 1.0 mM D-glucuronate for 2 days did not change significantly the catalytic activity or the content of the bound metal ion (data not shown). The apoenzyme could be reconstituted with other divalent cations, including $Mn^{2+}$, $Cd^{2+}$, $Co^{2+}$, or $Ni^{2+}$. The kinetic constants for the metal substituted variants of URI

Table 1: Kinetic Parameters and the Metal Content for the Metal-Reconstituted URI[a]

| metal | $k_{cat}$ ($s^{-1}$) | $K_m$ (mM) | $k_{cat}/K_m$ ($M^{-1}$ $s^{-1}$) | metal/URI | Zn/URI |
|---|---|---|---|---|---|
| apo | 180 ± 10 | 0.49 ± 0.05 | (3.6 ± 0.5) × $10^5$ | <0.05 | <0.05 |
| Zn | 190 ± 10 | 0.50 ± 0.05 | (3.8 ± 0.4) × $10^5$ | | 0.87 ± 0.05 |
| Mn | 210 ± 10 | 0.48 ± 0.04 | (4.3 ± 0.4) × $10^5$ | 0.81 ± 0.05 | 0.20 ± 0.03 |
| Co | 70 ± 2 | 0.30 ± 0.04 | (2.3 ± 0.3) × $10^5$ | 0.90 ± 0.05 | 0.08 ± 0.02 |
| Cd | 250 ± 10 | 0.55 ± 0.04 | (4.4 ± 0.3) × $10^5$ | 0.82 ± 0.05 | 0.07 ± 0.02 |
| Ni | 390 ± 10 | 8.5 ± 0.6 | (5.0 ± 0.3) × $10^4$ | 0.86 ± 0.05 | 0.10 ± 0.02 |

[a] These data were obtained at 30 °C, pH 8.0.

are, in general, very similar to the apoenzyme except for the Ni-URI, in which the Michaelis constant for D-glucuronate is increased about 20-fold. When uronate isomerase is expressed in *E. coli* in the absence of added divalent cations, the metal content of the purified protein was found to be 0.7 $Zn^{2+}$/subunit. The kinetic constants are listed in Table 1.

*Proton Exchange Catalyzed by Uronate Isomerase*. The mechanism of uronate isomerase was probed by incubating 10 $\mu$M enzyme and 5.0 mM D-glucuronate in 98% $D_2O$ and examining the changes in the $^1$H NMR spectra over a period of 24 h. Spectral differences were observed at the C1 and C2 proton resonances of α- and β-D-glucuronate. The C1 proton of α-D-glucuronate is coupled to the C2 proton with a $^3J$ value of 4.0 Hz, thus giving rise to a doublet at 5.094 ppm. After 8 h, the intensity of the doublet is decreased, and after 24 h the signal for the C1 proton appears as a singlet shifted slightly upfield. These spectral changes are shown in Figure 3A−C. Similar changes occur at the C1 $^1$H resonance of β-D-glucuronate (data not shown). These spectra illustrate the loss of vicinal proton coupling as a result of deuterium substitution at C2 of D-glucuronate. The incorporation of deuterium into the substrate was plotted as a function of time, and fit to a single-exponential rate equation yielded a rate constant of 0.13 $h^{-1}$. Correction of this value for the amount of enzyme and substrate gave a rate constant for exchange of 0.018 $s^{-1}$. Product turnover is thus 1.1 × $10^4$ fold faster than the exchange rate with solvent (196 $s^{-1}$/0.018 $s^{-1}$).

*Stereospecificity of the Uronate Isomerase Reaction*. During the conversion of D-glucuronate to D-fructuronate a hydrogen is transferred from C2 of D-glucuronate to either the *re*- or the *si*-face of the carbonyl carbon at C1. The stereospecificity of this transformation was determined by establishing whether the transferred hydrogen is subsequently found in either the *pro-S* or the *pro-R* position at C1 of the product D-fructuronate. The transferred hydrogen was specifically labeled with deuterium by first allowing the reaction to achieve isotopic equilibrium in $D_2O$. Unfortunately, the two methylene protons at C1 of D-fructuronate are indistinguishable by NMR due to small chemical shift differences and lack of vicinal proton coupling. The product D-fructuronate (**2**) was reduced enzymatically to D-mannonate (**3**) and then dehydrated by mannonate dehydratase to produce 2-keto-3-deoxy-D-gluconic acid (**4**). The deuterium transferred from C2 of D-glucuronate to C1 of D-fructuronate is thus ultimately found at C6 of 2-keto-3-deoxy-D-gluconic acid. The stereochemical assignment was determined via NMR spectroscopy from the size of the coupling constant to the single hydrogen at C5 since this sugar forms a stable pyranose ring structure (see Scheme 6).

The approximation of vicinal coupling constants using valence bond theory has been developed by Karplus (*21*). The distinction between the *pro-R* and *pro-S* protons on C6 of 2-keto-3-deoxy-D-gluconic acid (**13**) was ascertained by considering the magnitude of the coupling constants to the protons that are either cis or trans with the single vicinal proton on C5. It has been shown that vicinal protons with dihedral angles near 180°, as in the trans configuration, yield large coupling constants, whereas vicinal protons with dihedral angles near 60°, the cis configuration, yield smaller coupling constants. Models of 2-keto-3-deoxy-D-gluconic acid in the α-pyranose configuration (**14**) were constructed using Chem3D Ultra 8.0 and the MM2 version of the internal program. The model adopts a chair conformation with the axial *pro-S* proton on C6 trans to its vicinal neighbor, whereas the equatorial *pro-R* proton is cis. The calculated dihedral angles are 170° and 53°, respectively, and a representation of this conformation is shown in Scheme 6. The calculated coupling constants, obtained from eqs 3 and 4 are 8.9 and 2.7 Hz for the hydrogens at the *pro-S* and *pro-R* positions, respectively.

$$^3J = 8.5\cos^2\Phi - 0.28 \qquad (0° < \Phi < 90°) \quad (3)$$

$$^3J = 9.5\cos^2\Phi - 0.28 \qquad (90° < \Phi < 180°) \quad (4)$$

Four species of 2-keto-3-deoxy-D-gluconic acid exist in aqueous solution at pH 8 as determined by $^1$H NMR. The species and percentages are as follows: β-pyranose (49%), α-furanose (23%), β-furanose (17%), and α-pyranose (11%). The portion of the $^1$H NMR spectrum for the axial *pro-S* hydrogen in the fully protonated sample of the α-pyranose anomer of **14** is presented in Figure 4A. The chemical shift is 3.762 ppm, and coupling constants of 12 and 7.0 Hz are apparent to the *pro-R* hydrogen and the axial C5 hydrogen, respectively. For the equatorial *pro-R* hydrogen, coupling constants of 12 and 2.5 Hz are apparent to the *pro-S* hydrogen and axial C5 hydrogen, respectively, at a chemical shift of 3.529 ppm (data not shown). The values of these coupling constants are consistent with the computed values based upon the conformation of the α-pyranose anomer of **14**.

The D-[1-$^2H_1$]-fructuronate (**2**) was enzymatically converted to 2-keto-3-deoxy-D-[6-$^2H_1$]-gluconic acid (**4**). The region of the $^1$H NMR spectrum for the *pro-S* hydrogen of 2-keto-3-deoxy-D-[6-$^2$H]-gluconic acid (**4**) is presented in Figure 4B. The resonance for the *pro-S* hydrogen has been simplified to a doublet with a coupling constant of 7.0 Hz, and the chemical shift has moved upfield slightly to 3.743 ppm. The resonances are broadened because of the weak geminal coupling to the deuterium at the *pro-R* position. The resonance for the *pro-R* hydrogen was reduced to undetectable levels (data not shown). These results establish that during the enzymatic isomerization of D-glucuronate the proton is transferred to the *pro-R* position at C1 of D-fructuronate.

*Inhibition Studies*. Several compounds were tested as potential inhibitors of uronate isomerase. D-Arabinaric acid (**6**), D-arabinohydroxamate (**8**), and L-gulonic acid were found to be competitive inhibitors versus D-glucuronic acid. With both apo-URI and Zn-URI the $K_i$ value for **6** was found to be 13 ± 1 nM. With compound **8** the $K_i$ for the apo-URI was 930 ± 130 nM whereas with Zn-URI the $K_i$ was 670 ±

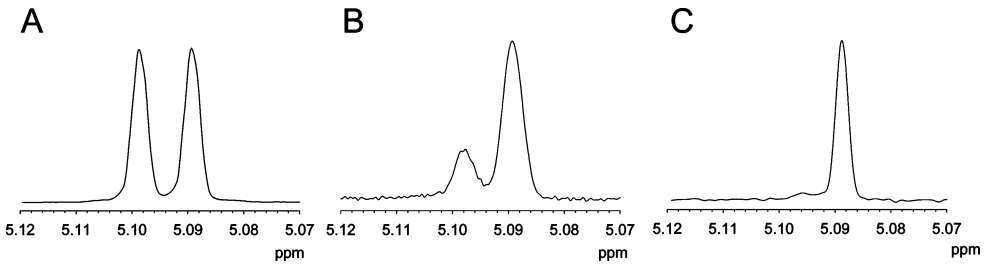


FIGURE 3: Spectral changes observed at $H_1$ of α-D-glucuronate after 0 h (A), 9 h (B), and 24 h (C) of incubation in 98% $D_2O$ with 10 $\mu$M uronate isomerase at pH 8.0. The initial D-glucuronate concentration was 5.0 mM.

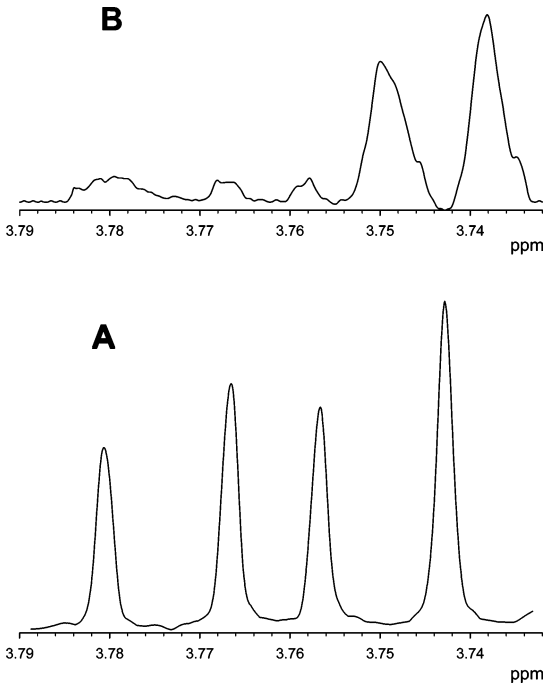


FIGURE 4: (A) $^1$H NMR spectrum of the *pro-S* hydrogen at C6 of the α-pyranose anomer of 2-keto-3-deoxy-D-gluconic acid (**14**). The geminal coupling constant to the *pro-R* hydrogen is 12 Hz, and the vicinal coupling constant to the lone proton at C5 is 7.0 Hz. (B) $^1$H NMR spectrum of the *pro-S* hydrogen at C6 of the α-pyranose anomer of [6-$^2H_R$]-2-keto-3-deoxy-D-gluconic acid (**4**). The vicinal coupling constant to the lone proton at C5 is 7.0 Hz.

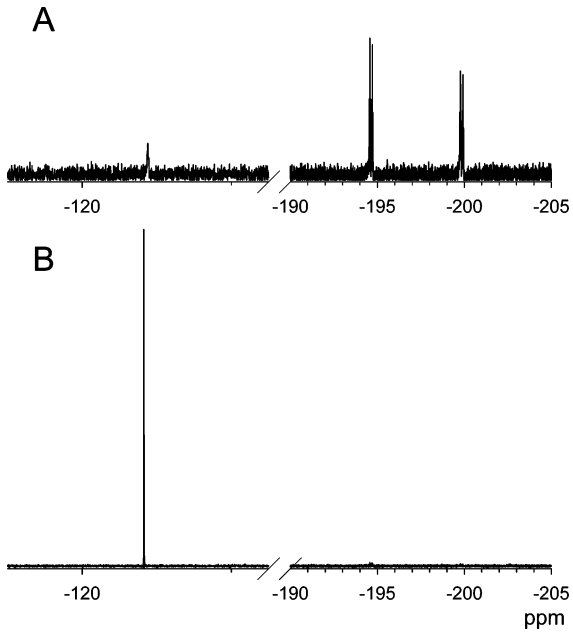


FIGURE 5: (A) $^{19}$F NMR spectrum of 10 mM 3-deoxy-3-fluoro-D-glucuronic acid (**12**) at pH 8.0 in the absence of URI. The free $F^-$ concentration was estimated to be 0.60 mM based upon the integration of the NMR signal for the fluoride at −120.9 ppm and the two anomers of **12** at −194.6 and −199.8 ppm. (B) $^{19}$F NMR spectrum of the reaction mixture after the addition of 0.1 $\mu$M URI to a 10 mM sample of **12** after 48 h. The concentration of $F^-$ increased to 8.9 mM, and the concentration of **12** was reduced to 1.1 mM.

Scheme 6

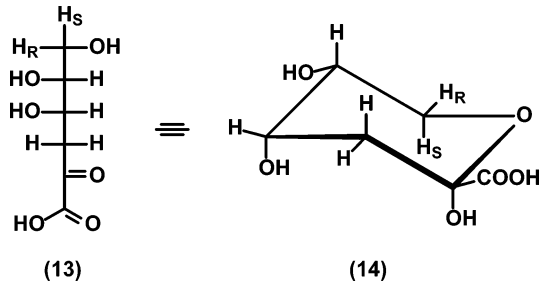


70 nM. L-Gulonic acid inhibited the Zn-URI with a $K_i$ of 430 ± 20 $\mu$M.

*Enzymatic Transformation of 3-Deoxy-3-fluoro-D-glucuronic Acid.* 3-Deoxy-3-fluoro-D-glucuronic acid was used to probe the presence of a carbanion intermediate species at C2 which may result in the elimination of fluoride. $^{19}$F NMR spectra were collected every 30 min for a sample containing 10 mM 3-deoxy-3-fluoro-D-glucuronic acid (**12**), 50 mM $P_i$, pD 8.0, and 0.1 $\mu$M URI. The concentration of fluoride increased from an initial value of 0.6 mM to >8.9 mM after 48 h of incubation with enzyme. In the absence of enzyme there was no increase in the fluoride concentration over a period of 48 h at pH 8.0. The $^{19}$F NMR spectrum of the reaction mixture before and after the addition of enzyme is presented in Figure 5. The rate of reaction was calculated by integration of the resonance for fluoride as a function of time. The minimum value of $k_{cat}$ for the defluorination of **12** is 0.85 $s^{-1}$. A proposal for the elimination of fluoride from **12** is presented in Scheme 7.

## DISCUSSION

*Proton Transfer Mechanism.* Uronate isomerase catalyzes the interconversion between D-glucuronate and D-fructuronate. The two most likely reaction mechanisms for this transformation require hydrogen migration between C2 and C1 of the substrate/product pair via a proton or hydride transfer (Scheme 2). These limiting reaction mechanisms can be differentiated from one another by an assessment of whether the enzyme is able to catalyze the exchange of the transferred hydrogen with solvent. With the hydride transfer mechanism no exchange is possible. However, the proton

Scheme 7

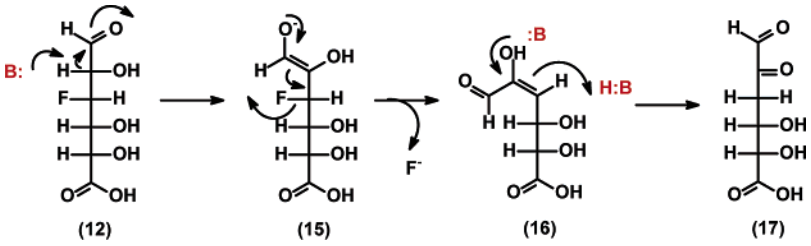


Scheme 8

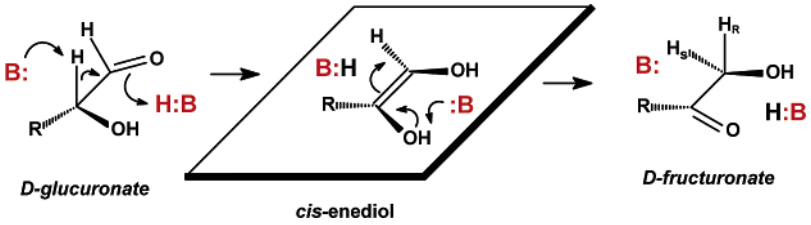


transfer mechanism can facilitate substrate/solvent exchange upon formation of the enediol intermediate and the appropriate conjugate acid. We have demonstrated that URI catalyzes the relatively slow, but stereospecific, exchange of solvent deuterium with substrate and product. These results are consistent with a proton transfer mechanism with a highly shielded conjugate acid. This exchange rate is significant, although it is slow in comparison to other enzymes which catalyze similar reactions via proton transfer mechanisms. Triosephosphate isomerase (TIM) catalyzes the exchange of the hydrogen at C2 of glyceraldehyde-3-phosphate at a rate that is about an order of magnitude faster than substrate/product interconversion (*12*). With phosphoglucose isomerase (PGI) the substrate/solvent exchange is about twice the rate of substrate/product interconversion (*22*). These differences in the rate of substrate/solvent exchange must be attributed to the accessibility of the conjugate acid in the active site with the external solvent and/or the relative concentration of the *cis*-enediol intermediate in the steady state. In contrast, the interconversion of substrate and product in xylulose isomerase is faster than the substrate/solvent exchange by 9 orders of magnitude (*15*).

The stereospecific transfer of the proton from C2 of D-glucuronate to C1 of D-fructuronate is supported by $^1$H NMR measurements which show that a single hydrogen is exchanged with solvent in the presence of URI. In the absence of enzyme neither the substrate nor the product exhibited any exchange with solvent after 1 month of incubation in $D_2O$. The stereochemical assignment of the transferred proton in D-fructuronate was achieved by enzymatic conversion of this product to 2-keto-3-deoxy-D-gluconic acid. The transferred proton was found in the *pro-R* position of the product thus establishing the stereospecific transfer of the D-glucuronate C2 proton to the *pro-R* position at C1 of D-fructuronate in the enzyme catalyzed isomerization. These data demonstrate that the transferred proton is added to the *re*-face of the C1 carbonyl of the substrate, which is consistent with the formation of a *cis*-enediol intermediate as shown in Scheme 8. A *cis*-enediol intermediate has been identified in all of the aldose−ketose isomerases that utilize a proton transfer mechanism.

Two mimics of the putative *cis*-enediol intermediate were shown to be potent inhibitors of URI. The relationship

Scheme 9

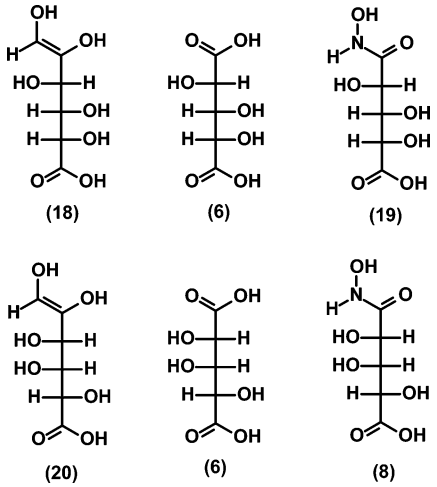


between the structure of the proposed intermediate and these compounds is presented in Scheme 9. URI from *E. coli* has previously been shown to catalyze the isomerization of either D-glucuronate or its C4 epimer, D-galacturonate (*18*). The *cis*-enediol intermediates for these two sugars are represented as structures **18** and **20**, respectively. D-Arabinaric acid (**6**) can function as a mimic of either intermediate, depending on the relative orientation of the two carboxylates when bound within the enzyme active site. This compound proved to be a very potent inhibitor of URI with a competitive inhibition constant of 13 nM. This result further supports the formation of an enediol intermediate in the isomerization of substrates by URI. The single hydroxamate derivative of D-arabinaric acid (**8**) that was made is an analogue of the enediol intermediate during the isomerization of D-galacturonate. Relative to D-arabinaric acid, the hydroxamate derivative binds less strongly to URI but the inhibitory properties also support a proton transfer mechanism and an enediol intermediate.

Similar compounds have been used previously to support proton transfer mechanisms in other aldose−ketose isomerases. A crystal structure of *Pyrococcus furiosus* PGI complexed with 5-phospho-D-arabinohydroxamate and 5-phospho-D-arabinonate supported a proton transfer mechanism through a *cis*-enediol intermediate (*23*). Inhibition studies of yeast

PGI with the same compounds yielded $K_i$ values of 230 nM and 2.1 $\mu$M, respectively (*24*). Phosphoglycolohydroxamate inhibits rabbit muscle TIM with a $K_i$ of 4 $\mu$M (*25*), and phosphoglycolate inhibits the same enzyme with a $K_i$ of 7 $\mu$M (*26*).

The utilization of a proton transfer mechanism is also supported by the enzyme catalyzed elimination of fluoride from 3-deoxy-3-fluoro-D-glucuronate. If the proton at C2 of the substrate can be abstracted with a suitably placed basic group within the active site of URI, the negative charge can be delocalized into the carbonyl at C1. Alternatively, the negative charge can be shifted toward C3 with expulsion of fluoride as presented in Scheme 7. The rate of fluoride elimination is approximately 1% that of the isomerization of D-glucuronate.

Similar results were obtained for glyoxylase I, which has been proposed to catalyze a proton transfer through a *cis*-enediol intermediate since fluoride was eliminated from fluoromethylglyoxal upon incubation with glyoxylase I (*27*). However, no elimination was observed upon the incubation of 3-deoxy-3-fluoro-D-glucose or 3-deoxy-3-fluoro-D-allose with D-xylose isomerase for up to 40 days (*15*). These data and the lack of a substrate/solvent exchange reaction have been used to support the hydride transfer mechanism for xylose isomerase (*15*, *16*).

The kinetic constants for URI are independent of whether a divalent cation is bound to the protein or not. Therefore, the catalytic activity of URI is not dependent on a divalent cation. URI is the first characterized member of the amidohydrolase superfamily that does not require a metal ion for enzymatic activity. It is obvious that URI from *E. coli* can bind up to one divalent cation, but the site of binding is uncertain. If the lone metal ion binds to the His-Xaa-His motif at the end of strand 1 of the $(\beta/\alpha)_8$ barrel, then it is likely that these histidine residues are not directly involved in the isomerization reaction. There are other examples from the amidohydrolase superfamily where metal binding to the $\alpha$-site is ambiguous. For example, in *N*-acyl D-amino acid deacetylase from *Alcaligenes faecalis*, a divalent cation must be bound to the $\beta$-site but a second divalent cation can bind to the $\alpha$-site. However, binding at that site is not essential for catalytic activity (*28*). In addition, approximately 40% of the annotated *N*-acetylglucosamine-6-phosphate deacetylases (NagA) have a Gln-Xaa-Asn motif at the end of strand 1 instead of the more common His-Xaa-His. Therefore, the essential nature of a bound metal at the $M_\alpha$-site in NagA is in doubt. The enzymatic activity of URI from *E. coli* does not require a divalent cation, and it is one of very few examples from the amidohydrolase superfamily that does not catalyze a hydrolytic reaction. These results highlight the extreme plasticity of the active sites found within the amidohydrolase superfamily of enzymes.

## ACKNOWLEDGMENT

We thank Professor John A. Gerlt for suggesting the use of mannonate dehydratase in the elucidation of the stereochemical course of uronate isomerase. We also thank Dr. Joseph Reibenspies for determining the structure of compound **8** via X-ray crystallography. Jessica Smith conducted some of the preliminary experiments with uronate isomerase.

## REFERENCES

1. Siebert, C. M., and Raushel, F. M. (2005) Structural and catalytic diversity within the amidohydrolase superfamily, *Biochemistry 44*, 6383−6391.
2. Holm, L., and Sander, C. (1997) An evolutionary treasure: unification of a broad set of amidohydrolases related to urease, *Proteins 28*, 72−82.
3. Aubert, S. A., Li, Y., and Raushel, F. M. (2004) Mechanism for the hydrolysis of organophosphates by the bacterial phosphotriesterase, *Biochemistry 43*, 5707−5715.
4. Benini, S., Rypniewski, W. R., Wilson, K. S., Miletti, S., Ciurli, S., and Mangani, S. (1999) A new proposal for urease mechanism based on the crystal structures of the native and inhibited enzyme from *Bacillus pasteurii*: Why urea hydrolysis costs two nickels, *Struct. Folding Des. 7*, 205−216.
5. Porter, T. N., Li, Y., and Raushel, F. M. (2004) Mechanism for the dihydroorotase reaction, *Biochemistry 43*, 16285−16292.
6. Wilson, D. K., Rudolph, F. B., and Quiocho, F. A. (1991) Atomic structure of adenosine deaminase complexed with a transition state analog: Understanding catalysis and immunodeficiency mutations, *Science 252*, 1278−1284.
7. Schwarzenbacher, R., Canaves, J. M., Brinen, L. S., Dai, X., Deacon, A. M., Elsliger, M. A., Eshaghi, S., Floyd, R., Godzik, A., Grittini, C., Grzechnik, S. K., Guda, C., Jaroszewski, L., Karlak, C., Klock, H. E., Koesema, E., Kovarik, J. S., Kreusch, A., Kuhn, P., Lesley, S. A., McMullan, D., McPhillips, T. M., Miller, M. A., Miller, M. D., Morse, A., Moy, K., Ouyang, J., Robb, A., Rodrigues, K., Selby, T. L., Spraggon, G., Stevens, R. C., van den Bedem, H., Velasquez, J., Vincent, J., Wang, X., West, B., Wolf, G., Hodgson, K. O., Wooley, J., and Wilson, I. A. (2003) Crystal structure of uronate isomerase (TM0064) from *Thermatoga maritima* at 2.85 Å resolution, *Proteins 53*, 142−145.
8. Pegg, S. C.-H., Brown, S., Ojha, S., Seffernick, J., Meng, E. C., Morris, J. H., Chang, P. J., Huang, C. C., Ferrin, T. E., and Babbitt, P. C. (2006) Leveraging enzyme structure−function relationships for functional inference and experimental design: the structure−function linkage database, *Biochemistry 45*, 2545−2555.
9. Topper, Y. J. (1957) On the mechanism of action of phosphoglucose isomerase and phosphomannose isomerase, *J. Biol. Chem. 225*, 419−426.
10. Rieder, S. V., and Rose, I. A. (1959) The mechanism of the triosphosphate isomerase reaction, *J. Biol. Chem. 234*, 1007−1010.
11. Harris, T. K., Cole, R. N., Comer, F. I., and Mildvan, A. S. (1998) Proton transfer in the mechanism of triosephosphate isomerase, *Biochemistry 37*, 16828−16838.
12. Herlihy, J. M., Maister, S. G., Albery, W. J., and Knowles, J. R. (1976) Energetics of triosephosphate isomerase: the appearance of solvent tritium in substrate dihydroxyacetone phosphate and in product, *Biochemistry 15*, 5607−5612.
13. O'Donoghue, A. C., Amyes, T. L., and Richard, J. P. (2005) Hydron transfer catalyzed by triosephosphate isomerase. Products of isomerization of (R)-glyceraldehyde-3-phosphate in $D_2O$, *Biochemistry 44*, 2610−2621.
14. O'Donoghue, A. C., Amyes, T. L., and Richard, J. P. (2005) Hydrogen transfer catalyzed by triosephosphate isomerase. Products of isomerization of dihydroxyacetone phosphate in $D_2O$, *Biochemistry 44*, 2622−2631.
15. Allen, K. N., Lavie, A., Farber, G. K., Glasfeld, A., Petsko, G. A., and Ringe, D. (1994) Isotopic exchange plus substrate and inhibition kinetics of D-xylose isomerase do not support a proton-transfer mechanism, *Biochemistry 33*, 1481−1487.
16. Fenn, T. D., Ringe, D., and Petsko, G. A. (2004) Xylose isomerase in substrate and inhibitor michaelis states: Atomic resolution studies of a metal-mediated hydride shift, *Biochemistry 43*, 6464−6474.
17. Tewson, T. J., and Welch, M. J. (1978) New approaches to the synthesis of 3-deoxy-3-fluoro-D-glucose, *J. Org. Chem. 43*, 1090−1092.
18. Ashwell, G., Wahba, A. J., and Hickman, J. (1960) Uronic acid metabolism in bacteria. I. Purification and properties of uronic acid isomerase in *Escherichia coli*, *J. Biol. Chem. 235*, 1559−1565.
19. Hickman, J., and Ashwell, G. (1960) Uronic acid metabolism in bacteria. II. Purification and properties of D-altronic Acid and D-mannonic acid dehydrogenases in *Escherichia coli*, *J. Biol. Chem. 235*, 1566−1570.

20. Bradford, M. M. (1976) A rapid and sensitive method for the quantitation of microgram quantities of protein utilizing the principle of protein-dye binding, *Anal. Biochem. 72*, 248−254.
21. Karplus, M. (1959) Contact electron-spin coupling of nuclear magnetic moments, *J. Chem. Phys. 30*, 11−15.
22. Rose, I. A., and O'Connell, E. L. (1961) Intramolecular hydrogen transfer in the phosphoglucose isomerase reaction, *J. Biol. Chem. 236*, 3086−3092.
23. Berrisford, J. M., Akerbroom, J., Brouns, S., Sedelnikova, S. E., Turnbull, A. P., van der Oost, J., Salmon, L., Hardré, R., Murray, I. A., Blackburn, G. M., Rice, D. W., and Baker, P. J. (2004) The structures of inhibitor complexes of *Pyrococcus furiosus* phosphoglucose isomerase provide insights into substrate binding and catalysis, *J. Mol. Biol. 343*, 649−657.
24. Hardré, R., Bonnette, C., Salmon, L., and Gaudemer, A. (1998) Synthesis and evaluation of a new inhibitor of phosphoglucose isomerases: the enediolate analogue 5-phospho-D-arabinohydroxamate, *Bioorg. Med. Chem. Lett. 8*, 3435−3438.
25. Collins, K. D. (1974) An activated intermediate analogue: The use of phosphoglycolohydroxamate as a stable analogue of a transiently occurring dihydroxyacetone phosphate-derived enolate in enzymatic catalysis, *J. Biol. Chem. 249*, 136−142.
26. Johnson, L. N., and Wolfenden, R. (1970) Changes in absorption spectrum and crystal structure of triose phosphate isomerase brought about by 2-phosphoglycollate, a potential transition state analogue, *J. Mol. Biol. 47*, 93−100.
27. Kozarich, J. W., Chari, R. V. J., Wu, J. C., and Lawrence, T. L. (1981) Fluoromethylglyoxal: Synthesis and glyoxalase I catalyzed product partitioning via a presumed enediol intermediate, *J. Am. Chem. Soc. 103*, 4593−4595.
28. Liaw, S. H., Chen. S. J., Ko, T. P., Hsu, C. S., Chen, C. J., Wang, A. H. J., and Tsai, Y. C. (2003) Crystal structure of D-aminoacylase from *Alcaligenes faecalis* DA1. A novel subset of amidohydrolases and insights into the enzyme mechanism, *J. Biol. Chem. 278*, 4957−4962.

BI060531L